MIXED CONVECTION IN AN ECCENTRIC ANNULUS FILLED BY COPPER NANOFLUID

by

Wael El-MAGHLANY[a*], Mohamed ABO ELAZM[b], Ali SHAHATA[b], and Yehia ELDRAINY[a]

[a] Faculty of Engineering, Alexandria University, Alexandria, Egypt
[b] Arab Academy for Science and Technology and Maritime Transport, Alexandria, Egypt

Original scientific paper
DOI:10.2298/TSCI140802128E

A numerical study of mixed convection flow and heat transfer of copper-water nanofluid inside an eccentric horizontal annulus is presented. The inner and outer cylinders are kept at constant temperatures as T_h and T_c, respectively. The inner cylinder rotates to generate the forced convection effect. The numerical work was carried out using an in-house CFD code written in FORTRAN. Different scenarios were explored to explain the effects of different parameters on the studied problem. These parameters are Richardson number, eccentricity ratio, and solid volume fraction. The range of the Richardson number, solid volume fraction of the nanoparticles, and the eccentricity ratio, are $0.01 \leq Ri \leq 100$ (natural convection), $0 \leq \zeta \leq 0.05$, $0 \leq \varepsilon \leq 0.9$, respectively. All results were performed with thermal Grashof number, and radius ratio Rr, equaled to 10^4 and 2, respectively. The effects of eccentricity, nanoparticles volume fraction, and Richardson number on the average Nusselt number, streamlines and isotherms were investigated. Results were discussed, and were found to be in good agreement with previous works. It was also found that, the eccentricity has a positive remarkable effect on the average Nusselt number, while the effect of nanoparticles concentration was more pronounced at mixed convection region (Ri = 1).

Key words: *mixed convection, eccentric annulus, nanofluid, numerical study*

Introduction

Mixed convection heat transfer inside annular spaces was the subject of many theoretical and experimental studies due to its great importance in many engineering applications, such as heat exchangers, journal bearing, electrical motor and generator, thermal storage systems and cooling of electronic components. The effect of eccentricity has become an area of interest where many researchers try to study its effect on heat transfer. The tube in tube heat exchanger is one of the applications of heat transfer inside annular spaces, but the minuscule surface area stand as an obstacle to high capacity heat transfer applications, many trials were performed to enhance the heat transfer capacity such as rotation of the inside or the outside tube. The present study was focused on the enhancement of heat transfer due to eccentricity, nanoparticles addition to the working fluid, and the rotation of the inner tube. Enhancement of heat transfer with nano particles has recently a great attention [1, 2]. Numerical simulation of natural convection in concentric and eccentric circular cylinder has been reported in the litera-

* Corresponding author; e-mail: elmaghlany@alexu.edu.eg

tures [3-8]. Bau [9] studied the thermal convection in a saturated porous medium confined between two horizontal eccentric cylinders by the use of a regular perturbation expansion in terms of the Darcy-Rayleigh number; it was found that the proper choice of eccentricity values can optimize the heat transfer inside annulus which has a bearing on the design of different thermal insulators. A literature review on the general heat transfer characteristics of nanofluids has been conducted recently by Trisaksri and Wongwises [10], and Wang and Mujumdar [11]. Khanafer *et al*. [12] studied the use of copper-water nanofluid in a 2-D rectangular enclosure. They found a significant increase in the heat transfer rate by increasing the percentage of the suspended particles. Higher thermal conductivity can be achieved in thermal systems using nanofluids as shown by Eastman *et al*. [13] and Xie *et al*.[14]. The addition of a one percent by volume of nanoparticles to usual fluids increases the thermal conductivity of the fluid up to approximately two times as determined by Choi *et al*. [15]. Natural convection of nanofluid in a concentric annulus considering variable viscosity and variable thermal conductivity has been investigated by Abu-Nada [16] and Abu-Nada *et al*. [17]. Matin and Pop [18] studied numerically natural convection flow and heat transfer of copper (Cu)-water nanofluid inside an eccentric horizontal annulus, they investigated the effects of the eccentricity, radii ratio, the nanoparticles volume fraction parameter, the Rayleigh number, and the Prandtl number on the mean Nusselt number. Laminar mixed convection Al_2O_3-water nanofluid flow in elliptic ducts with constant heat flux boundary condition has been simulated employing two phase mixture model by Shariat *et al*. [19]. Results showed that in a given Reynolds number and Richardson number, increasing solid nanoparticles volume fraction increases the Nusselt number while the skin friction factor decreases. Increasing aspect ratio in elliptic tubes reduces the local skin friction factor whereas it does not have any specified effect on the local Nusselt number. Mirmasoumi and Behzadmehr [20] studied numerically laminar mixed convection of a nanofluid consisting of water and Al_2O_3 in a horizontal tube. Two-phase mixture model has been used to investigate hydrodynamic and thermal behaviors of the nanofluid over a wide range of the Grashof and Reynolds numbers. The results showed that at the fully developed region the nanoparticle concentration does not have significant effects on the hydrodynamics parameters. However, its effects on the thermal parameters are important. Concentration of the nanoparticles is higher at the bottom of the tube and also at the near wall region. Fully developed laminar mixed convection of a nanofluid consisting of water and Al_2O_3 in a horizontal curved tube has been studied numerically by Akbarinia and Behzadmehr [21]. Simultaneous effects of the buoyancy force, centrifugal force and nanoparticles concentration has been presented. The nanoparticles volume fraction does not have direct effects on the secondary flow, axial velocity and the skin friction coefficient. However, its effects on the entire fluid temperature could affect the hydrodynamic parameters when the order of magnitude of the buoyancy force becomes significant compared to the centrifugal force. Kalteha *et al*. [22] studied both numerically and experimentally the laminar convective heat transfer of an alumina-water nanofluid flow inside a wide rectangular microchannel heat sink. Decent investigation in the same way of the present study was performed by Habibi Matin and Pop [23]; they introduced a numerical study of mixed convection flow and heat transfer of Al_2O_3-water nanofluid inside an eccentric horizontal annulus with rotation on the inner cylinder. From the previous survey it was noted that there are no investigations concerned with the convection utilizing nanofluid in eccentric annulus except the performed investigations by Habibi Matin and Pop [18, 23]. Habibi Matin and Pop [18] only concerned with natural convection not mixed convection. The present study is an extension to the work of Habibi Matin and Pop [23] but with different nano type (Cu instead of Al_2O_3) and different Reynolds number with constant Rayleigh number led to mixed convection heat transfer mode. The results will be introduced as an enhancement in Nusselt number due to both eccentricity and nano concentrations for different Reynolds number which is the main object of the present study.

Mathematical formulation

The steady-state 2-D laminar mixed convection of Cu-water nanofluid in annuli of eccentric horizontal cylinders of radii r_i and r_0 is considered as shown in fig. (1). The outer cylinder is cooled at temperature T_c and the inner cylinder is kept at the hot temperature T_h. The eccentricity was considered below the center of the outer cylinder. The temperature gradient generates the natural convection while the inner cylinder is considered able to rotate to create the forced convection effect. It was also assumed that, the base fluid and nanoparticles are in thermal equilibrium, the nanofluid is Newtonian and incompressible, and the flow is laminar. The thermo-physical properties of the base fluid and the nanoparticles are given in tabs. 1 and 2.

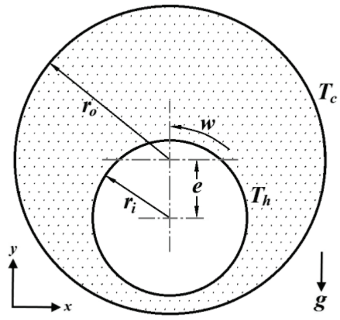

Figure 1. Physical model of eccentric annulus

The thermal transport in nanofluids can be grouped into two categories. First one take the particle dynamics into consideration, whose effect is additive to the thermal conductivity of a static dilute suspension. Thus, the particle size, volume fraction, thermal conductivities of both the nanoparticle and the base fluid, and the temperature itself are taken into account in such models for the thermal conductivity of nanofluids. The second one has started from the nanostructure of nanofluids by assuming that the nanofluid is a composite, formed by the nanoparticle as a core, and surrounded by a nanolayer as a shell, which in turn is immersed in the base fluid, and from which a three-component medium theory for a multiphase system is developed.

Table 1. Thermo-physical properties of pure water and nanoparticles

Physical properties	Pure water	Cu
ρ [kgm^{-3}]	997.1	8933
C_P [Jkg^{-1}K^{-1}]	4179	385
K [Wm^{-1}K^{-1}]	0.613	400
β [K^{-1}]	$21\cdot10^{-5}$	$1.67\cdot10^{-5}$

Table 2. Applied formulation of nanofluids properties

Nanofluids properties	Applied model
Density	$\rho_{nf} = (1-\zeta)\rho_f + \zeta\rho_s$
Thermal diffusivity	$\alpha_{nf} = k_{nf}/(\rho C_p)_{nf}$
Heat capacitance	$(\rho C_p)_{nf} = (1-\zeta)(\rho C_p)_f + \zeta(\rho C_p)_s$
Thermal expansion coefficient	$(\rho\beta)_{nf} = (1-\zeta)(\rho\beta)_f + \zeta(\rho\beta)_s$
Dynamic viscosity	$\mu_{nf} = \dfrac{\mu_f}{(1-\zeta)^{2.5}}$
Thermal conductivity	$k_{nf} = k_f \left[\dfrac{(k_s+2k_f)-2\zeta(k_f-k_s)}{(k_s+2k_f)+\zeta(k_f-k_s)}\right]$

Constant thermo-physical properties were considered for the nanofluid except for the density variation in the buoyancy forces which was determined using the Boussinesq approximation.

$$\rho = \rho_o\left[1-\beta\left(T-T_c\right)\right] \tag{1}$$

where β is the coefficient for thermal expansion such that:

$$\beta = -\frac{1}{\rho_0}\left(\frac{\partial\rho}{\partial T}\right)_{P=C} \tag{2}$$

The governing equations for the problem under consideration are based on the balance laws of mass, linear momentum and thermal energy in two dimensions steady-state.

To put the governing equations in the dimensionless form, the following dimensionless variables are introduced to the governing equations:

$$V_r = \frac{v_r}{\omega r_i}, \quad V_\phi = \frac{v_\phi}{\omega r_i}, \quad R = \frac{r}{b}, \quad \theta = \left(\frac{T - T_c}{T_h - T_c}\right), \quad P = \frac{p}{\rho_{nf}(\omega r_i)^2}, \quad Rr = \frac{r_0}{r_i},$$
$$\varepsilon = \frac{e}{b}, \quad \mathrm{Re} = \frac{\omega r_i b}{\nu_f}, \quad \mathrm{Gr} = \frac{g\beta_f \Delta T b^3}{\nu_f^2}, \quad \mathrm{Pr} = \frac{\nu_f}{\alpha_f}, \quad \mathrm{Ri} = \frac{\mathrm{Gr}}{\mathrm{Re}^2} \tag{3}$$

The dimensionless form of the governing equations for continuity, momentum, and energy in ν cylindrical co-ordinate are:

$$\left(\frac{\partial V_r}{\partial R} + \frac{V_r}{R} + \frac{\partial V_\phi}{R\partial\phi}\right) = 0 \tag{4}$$

$$\left(V_r \frac{\partial V_r}{\partial R} + V_\phi \frac{\partial V_r}{R\partial\phi} - \frac{V_\phi^2}{R}\right) = -\frac{\partial P}{\partial R} - \frac{(\rho\beta)_{nf}}{\rho_{nf}\,\beta_f} Ri\theta\cos\phi +$$
$$+\frac{1}{\mathrm{Re}}\frac{\rho_f\,\mu_{nf}}{\rho_{nf}\,\mu_f}\left(\frac{\partial^2 V_r}{\partial R^2} + \frac{1}{R}\frac{\partial V_r}{\partial R} - \frac{V_r}{R^2} + \frac{\partial^2 V_r}{R^2\partial\phi^2} - \frac{2}{R^2}\frac{\partial V_\phi}{\partial\phi}\right) \tag{5}$$

$$\left(V_r \frac{\partial V_\phi}{\partial R} + V_\phi \frac{\partial V_\phi}{R\partial\phi} + \frac{V_r V_\phi}{R}\right) = -\frac{\partial P}{R\partial\phi} + \frac{(\rho\beta)_{nf}}{\rho_{nf}\,\beta_f} Ri\,\theta\sin\phi +$$
$$+\frac{1}{\mathrm{Re}}\frac{\rho_f\,\mu_{nf}}{\rho_{nf}\,\mu_f}\left(\frac{\partial^2 V_\phi}{\partial R^2} + \frac{1}{R}\frac{\partial V_\phi}{\partial R} - \frac{V_\phi}{R^2} + \frac{\partial^2 V_\phi}{R^2\partial\phi^2} + \frac{2}{R^2}\frac{\partial V_r}{\partial\phi}\right) \tag{6}$$

$$\left(V_r \frac{\partial\theta}{\partial R} + V_\phi \frac{\partial\theta}{R\partial\phi}\right) = \frac{k_{nf}}{k_f}\frac{(\rho C_p)_f}{(\rho C_p)_{nf}}\frac{1}{\mathrm{Re\,Pr}}\left[\frac{1}{R}\frac{\partial}{\partial R}\left(R\frac{\partial\theta}{\partial R}\right) + \frac{\partial^2\theta}{R^2\partial\phi^2}\right] \tag{7}$$

For the boundary conditions, the temperature is maintained by considering higher magnitude at the inner cylinder. In addition, the outer cylinder is fixed but the inner cylinder is assumed to rotate in anti-clockwise. The dimensionless boundary conditions:

$$V_\phi = 1, \ V_r = 0, \ \theta = 1.0, \ \text{at} \ R = R_i \tag{8}$$

$$V_\phi = 0, \ V_r = 0, \ \theta = 0, \ \text{at} \ R = R_\mathrm{o} \tag{9}$$

By defining the Nusselt number as the ratio between the actual heat transfer rate and the heat transferred by pure conduction, the local Nusselt number along the inner cylinder is calculated as:

$$\mathrm{Nu}_x = \frac{k_{nf}}{k_f}\ln\left(\frac{R_i}{R_o}\right) \times \left(R\frac{\partial\theta}{\partial R}\right)_{R=R_i} \tag{10}$$

The average Nusselt number is calculated by integrating the local value over the entire circumference of the inner cylinder as follows:

$$\mathrm{Nu} = \frac{1}{2\pi}\int_0^{2\pi} \mathrm{Nu}_x \,\mathrm{d}\phi \tag{11}$$

Numerical code details

The governing equations were solved by using the finite volume technique developed by Patankar [21]. This technique was based on the discretization of the governing equations using the central differencing in space. This solver, which was developed in FORTRAN, was used by the author El-Maghlany [22-25] in numerous other studies, where more detailed description of the solver and its validation measures were presented [26-28]. The effect of the number of grids on the solution was examined; tab. 3 represents the mesh sizes and fig. 2 shows the effect of number of grid on the solution. Through this study, a domain size of (90 × 70) was used. The discretization equations were solved by the Gauss–Seidel method. The iteration method used in this program is a line-by-line procedure, which is a combination of the direct method and the resulting tri-diagonal-matrix-algorithm (TDMA). The convergence of the solution was approached when the change in the average Nusselt as well as other dependent variables through one hundred iterations was found to be less than 0.01% from its initial value has been used as shown in fig. (2).

Table 3. Details of the five grids used in the grid independency study

Grid No.	Domain size
M-1	11 × 6
M-2	22 × 17
M-3	45 × 35
M-4	90 × 70
M-5	120 × 100

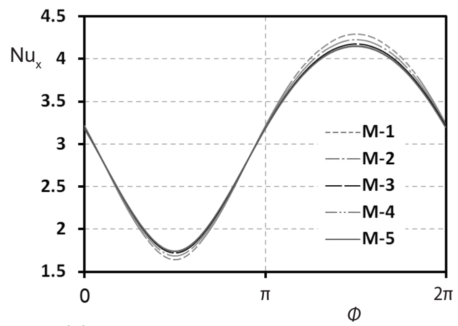

(a)

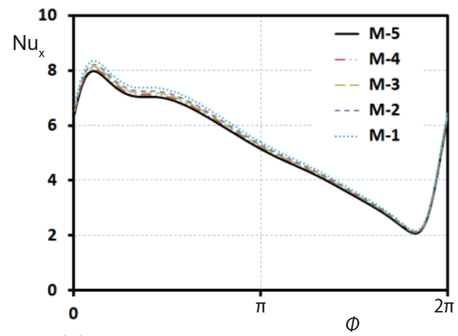

(b)

Figure 2. Variation of local Nusselt number for five different grids; (a) $\varepsilon = 0$, Ra = 10^4, and Pr = 0.7 (b) $\varepsilon = 0.9$, Ri = 0.1, and Pr = 6.13

Program validation and comparison with previous work

In order to check the accuracy of the numerical solution technique employed for the present study, it was validated with the results reported by Abu-Nada *et al.* [17] and Habibi Matin and Pop [18] for concentric annulus $\varepsilon = 0$, $\zeta = 0$, $Rr = 2.5$ and Pr = 0.7 for the average Nusselt number and is represented in fig. 3(a). Another validation with the results reported by Habibi Matin and Pop [23] for the average Nusselt number with nanofluid for concentric annulus, Re = 150, $\varepsilon = -0.34$, $Rr = 2.5$, Ra = 10^4 and Pr = 6 and is represented in fig. 3(b). The figure shows a good agreement between the present code and their results.

Results and discussion

Different scenarios were explored to explain the effects of different parameters on the studied problem. These parameters are Richardson number, eccentricity ratio, and solid volume fraction. The range of the Richardson number, solid volume fraction of the nanoparticles ζ, and the eccentricity ratio ε, are $0.01 \le \mathrm{Ri} \le 100$ (natural convection), $0 \le \zeta \le 0.05$, and $0 \le \varepsilon \le 0.9$, respec-

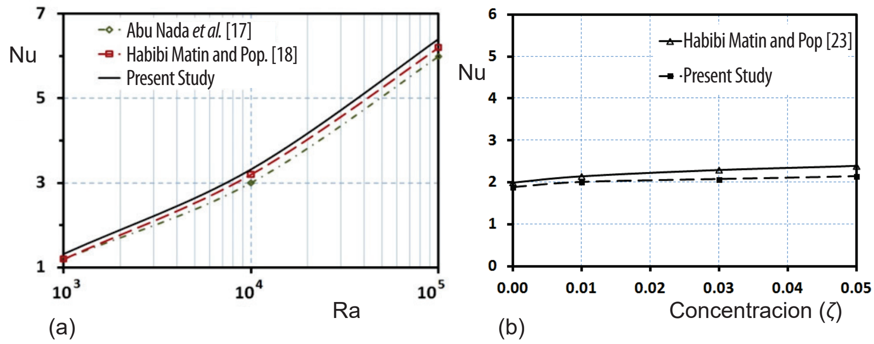

Figure 3. (a) Comparison between the present results for average Nu with the results reported by Abu-Nada *et al.*[17] and Habibi Matin and Pop [18]; (b) Comparison between the present results for average Nu with the results reported by Habibi Matin and Pop [23]

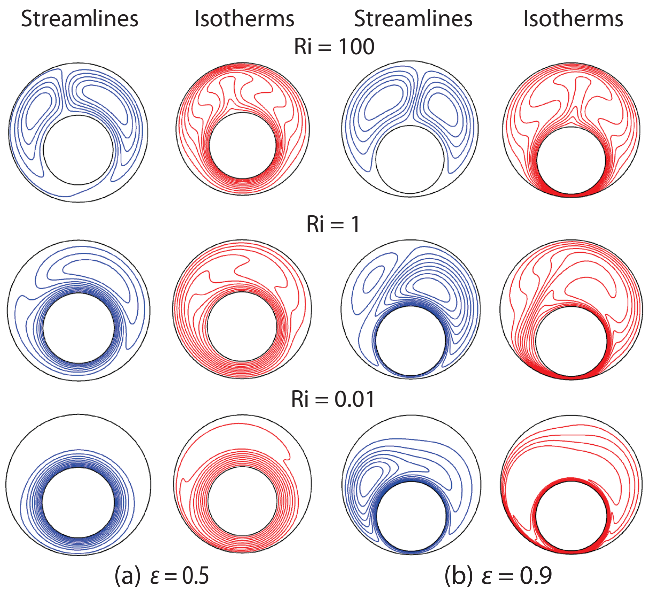

Figure 4. Streamlines and isotherms when $\zeta = 0$ and Pr = 6.13

tively. The Prandtl number is set to 6.13 representing water. All results were performed with thermal Grashof number, and radius ratio *Rr*, equaled to 10^4 and 2, respectively. The effect of the Richardson number on the streamlines and isotherms is shown in figs. 4 to 6 for eccentricity ratio of 0.5 and 0.9 while the solid volume fraction of the nanoparticles are 0, 0.01, and 0.05. The same trend was found for different solid volume fraction of the nanoparticles, but it is clear that by increasing the volume fraction of nanoparticles, the magnitudes of streamlines contours are reduced due to the increased viscosity of the nanofluids, mainly at high values of Richardson number (natural convection domain), on the other hand, the enhancement in fluid thermal conductivity by the addition of nanoparticles led to progressive augmentation in heat transfer coefficient depending on Richardson number. For higher values of Richardson number (Ri =100), the flow is supposed to be induced by the buoyancy force sustained by the temperature gradient. The streamlines consists of one pair of cells, one at the right and the other one at the left side of annulus. The two cells are not similar in shape except in pure natural convection mode. Since in the right portion the forced flow assisted the natural flow, on the other hand for the left portion, the two streams opposing each other, the right cell is stronger than the left cell. This destroys both the similarity of the two cell shapes and their symmetry. The separation line of $\psi = 0$ which separates the two large eddies moves in the direction of the cylinder rotation for $\varepsilon = 0.5$ (small eccentricity ratio), but at $\varepsilon = 0.9$, the gap above the inner cylinder becomes large and the natural convection effect attracts the streamlines towards the above cold cylinder. Both eddies circulate in the opposite direction to each other. The right cell rotates counter clockwise, while the eccentricity ratio had significant effect. For $\varepsilon = 0.5$, the gap down the inner cylinder is reduced in counter with the upper one and consequently elimination of streamlines down the inner cylinder is evidently remarkable as the eccentricity increased to $\varepsilon = 0.9$, but the stream lines collapsed above inner cylinder. As Richardson number decreased, the effect of forced flow is pronounced. At Ri = 1, the mixed convection is dominated, the right eddy becomes much bigger and fills the right portion of the annulus but is also deflected to the left at the top of the annulus due to the effect of the drag force. As Ri decreases, the viscous force drags the two cells in the direction of the cylinder rotation. At Ri = 0.1, the left eddy disappears and the flow pattern moves from two eddies towards one eddy and the separation line encompasses the large eddy again. At Ri = 0.01, the forced flow is dominated, the remaining eddy disappears and the flow regime moves from one eddy towards no-eddy. The flow pattern becomes concentric circles around the inner cylinder, but at $\varepsilon = 0.9$ there is free space above the inner cylinder stretching the stream lines to the outer surface in this region. This distribution is similar to the couette flow patterns at zero eccentricity. The flow strength is very high close to the inner cylinder. Conversely, it is very weak nearer the outer cylinder. On the other hand, and for high Richardson number, the isotherms are represented by the thermal plume which appears over the inner cylinder and very closed isotherms under the inner cylinder which represented high rates of heat transfer mainly at $\varepsilon = 0.9$. As Richardson number decreases, the thermal plume rotates in the di-

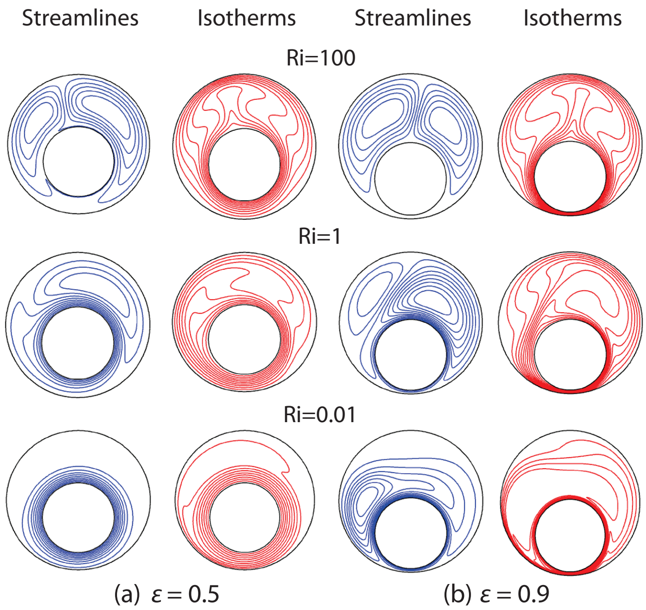

Figure 5. Streamlines and isotherms, ζ = 0.01

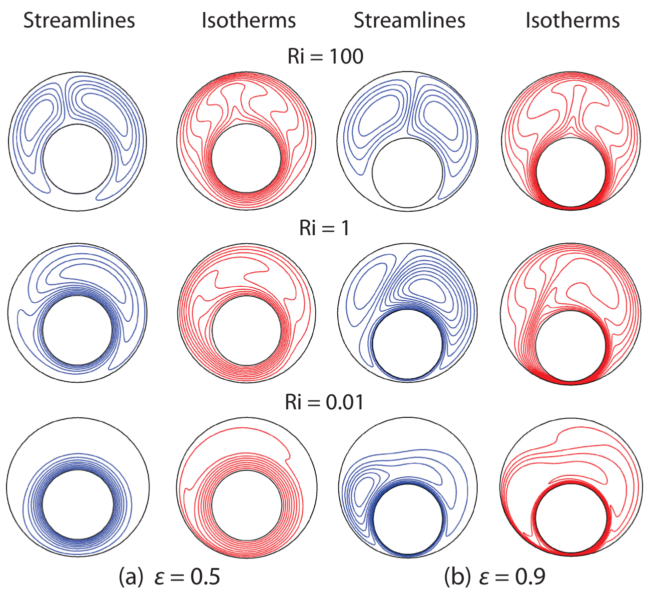

Figure 6. Streamlines and isotherms, ζ = 0.05

rection of the cylinder rotation at $\varepsilon = 0.5$ and gets bigger in size but at $\varepsilon = 0.9$ the plume is attracted to the outer cylinder due to free space for the natural convection domain above the cylinder. As Richardson number decreases to 0.01 (dominated forced convection regime), isotherms become almost concentric rings around the inner cylinder with high concentration as the eccentricity ratio increased. This led to high heat transfer rate. The effect of eccentricity ratio on the average Nusselt number for clear fluid and nanofluids is given in figs. 7 and 8 for different Richardson number. As shown, at a specified Richardson number as the eccentricity increased downward the average

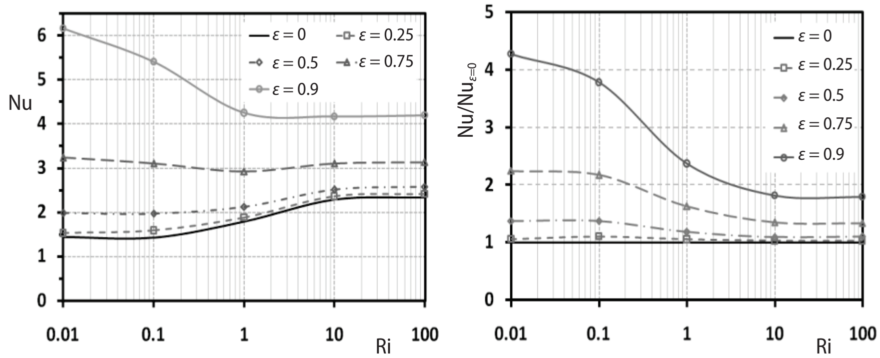

Figure 7. Average Nusselt number and its augmentation for eccentric annulus, $\zeta = 0$, and Pr = 6.13

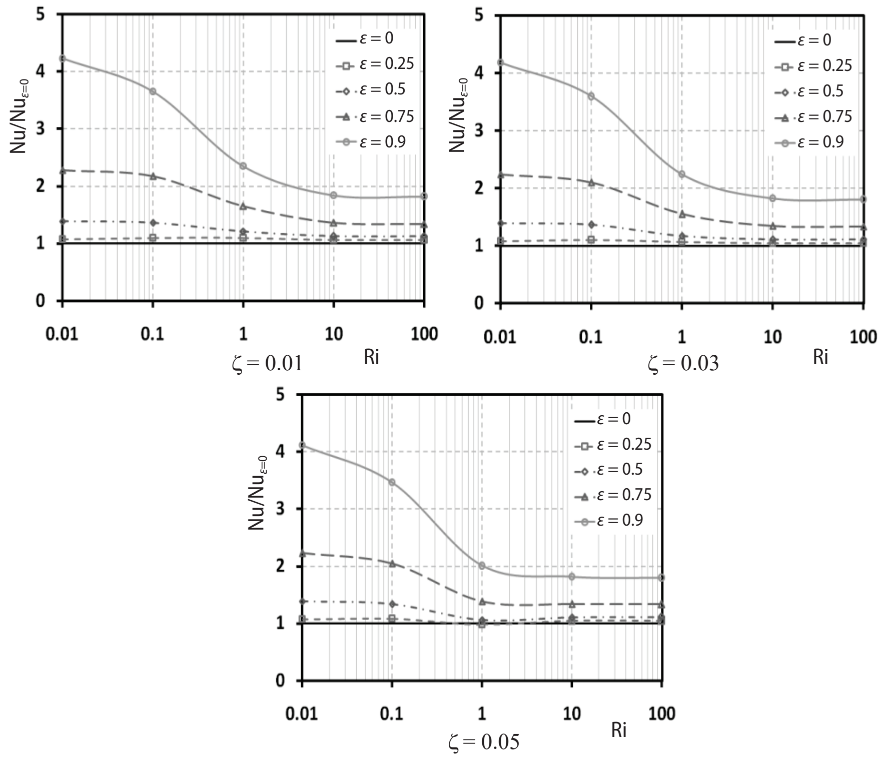

Figure 8. Augmentation of Nusselt number for eccentric annulus at different solid volume concentration

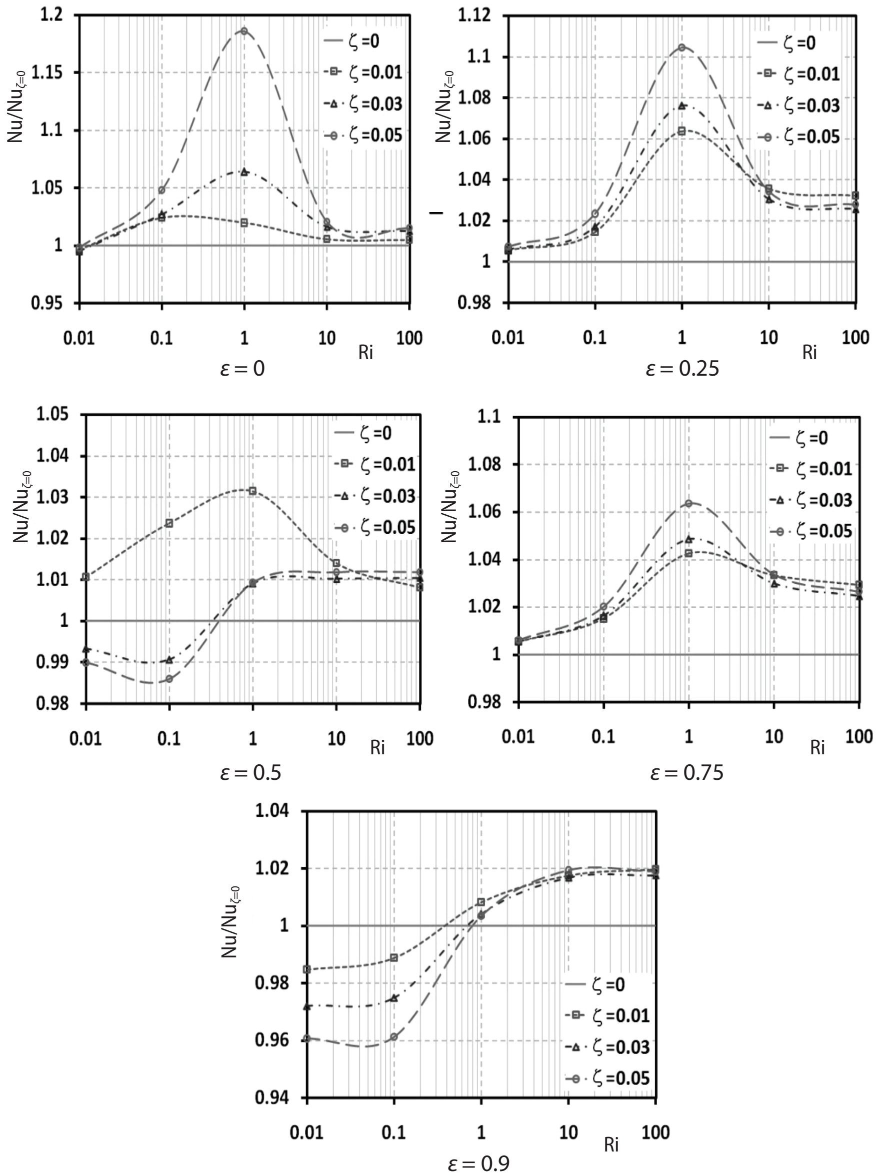

Figure 9. Augmentation of Nusselt number for eccentric annulus at different eccentricity ratio

Nusselt number increased, this is due to the upper gap between the cylinders becoming large thus maximizing the fluid convection inside the annulus and the fluid moves freely at the top of the inner cylinder. This is observed clearly at low values of Richardson number (forced convection mode) due to the assisting between both natural and forced convection. Figures 7 and 8 also represented the augmentation of the average Nusselt number due to the eccentricity, the figure showed significant augmentation in average Nusselt number in forced convection domain (low Richardson number values) decreased gradually as Richardson number increased (natural convection domain) but the eccentricity still enhanced the heat transfer. The effect of nanoparticals concentration does not change the effect of the eccentricity ratio on the average Nusselt number and also the augmentation in heat transfer character, but only on the amount of this augmentation. It was observed from fig. 9 that for concentric tubes ($\varepsilon = 0$) the addition of nanoparticals depends strongly on the value of Richardson number (heat transfer mode), no augmentation in heat transfer for both forced or natural convection but only good augmentation in the mixed convection mode (Ri = 1). As the eccentricity increased the peak enhancement in the heat transfer decreased gradually to reach the minimum one at $\varepsilon = 0.9$ at natural convection mode (Ri = 100) with respect to the other eccentricity ratio ($\varepsilon = 0, 0.25, 0.5, 0.75$). A good observation was found at high eccentricity in fig. 9. At low value of Richardson number (Ri = 0.01), the high eccentricity value ($\varepsilon = 0.9$) led to enhancement in heat transfer but only in the absence of nanoparticals, in contrary the enhancement in heat transfer will be in the natural convection domain (Ri ≥ 10) at all concentration values.

Conclusions

In this paper the influence of eccentricity, nanoparticle volume fraction, and Richardson number on the average Nusselt number, streamlines, and isotherms have been studied for an eccentric annulus filled with copper (Cu)-water based nanofluid, and the following conclusions were found.

- Results clearly indicated that the addition of copper nanoparticles has produced a extraordinary enhancement on heat transfer with respect to that of the pure fluid depending on the value of Richardson number, the effect of nanoparticles concentration on the average Nusselt number is more pronounced at mixed convection mode (Ri = 1) which increases appreciably with an increase of nanoparticles volume fraction parameter with optimum augmentation at zero eccentricity.
- It can be noted that the eccentricity has a positive remarkable effect on the average Nusselt number, this remarkable enhancement established at low Richardson number but in the absence of nanoparticals.
- The addition of nanoparticles does not necessarily enhance the heat transfer but there are restrictions depending on the other parameters.
- Brownian motion and thermophoresis effects in nanofluid heat transfer enhancement will be taken into account in future work. Brownian motion effect is remarkable in natural convection heat transfer. In the present work for mixed convection the Brownian motion has minor effect on the Nusselt number, the Nusselt number will be changed but with the same behavior as the prrsented values.
- More investigations are needed to understand the physical phenomenon of nanoparticals addition completely before using these fluids in practical cooling applications.

Nomenclature

b – annulus gab width, [r_0-r_i], [m]
C_p – specific heat at constant preassure, [Jkg^{-1}K^{-1}]
e – eccentricity, [m]
Gr – thermal Grashof number, [–]
g – acceleration of gravity, [ms^{-2}]
h – heat transfer coefficient, [Wm^{-2}K^{-1}]
k – fluid thermal conductivity, [Wm^{-1}K^{-1}]
Nu – average Nusselt number, [–]
Nu_x – local Nusselt number, [–]
P – dimensionless pressure, [–]
Pr – Prandtl number, [–]
p – pressure, [Nm^{-2}]
R – dimensionless radial co-ordinates, [–]
Ra – thermal Rayleigh number, [–]
Re – rotational Reynolds number, [–]
Ri – Richardson number, [–]
Rr – radius ratio, [–]
r – radial co-ordinate, [–]
r_i, r_o – inner and outer radii, respectively, [m]

T – local temperature, [K]
T_c – temperatures at outer radius, [K]
T_h – temperatures at inner radius, [K]
ΔT – temperature difference, [$T_h - T_c$], [K]
v_r – velocity in r-direction, [ms^{-1}]
v_φ – velocity in φ-direction, [ms^{-1}]

Greek symbols

α – thermal diffusivity, [m2s^{-1}]
β – coefficient of thermal expansion, [K^{-1}]
ε – eccentricity ratio, [–]
ζ – solid volume fraction, [–]
θ – dimensionless temperature, [–]
ν – kinematic viscosity, [m^{2}s^{-1}]
ρ – density, [kgm^{-3}]
ψ – dimensionless stream function, [–]
ω – angular velocity, [rad s^{-1}]
ϕ – angular co-ordinate, [–]

Subscript

f – fluid
o – reference
s – Solid

References

[1] Mahmoodi, M., *et al.*, Free Convection of a Nanofluid in a Square Cavity with a Heat Source on The Bottom Wall and Partially Cooled From Sides, *Thermal Science, 18* (2014), Suppl. 2, pp. S283-S300
[2] Mahmoodi, M., Mixed Convection Inside Nanofluid Filled Rectangular Enclosures with Moving Bottom Wall*, Thermal Science, 15* (2011), 3, pp. 889-903
[3] Deng, Q., Fluid Flow and Heat Transfer Characteristics of Natural Convection in Square Cavities Due to Discrete Source Sink Pairs, *Int. J. Heat Mass Transfer, 51* (2008), 25-26, pp. 5949-5957
[4] Mohamad, A., Kuzmin, A., A Critical Evaluation of Force Term in Lattice Boltzmann Method, Natural Convection Problem, *Int. J. Heat Mass Transfer, 53* (2010), 5-6, pp. 990-996
[5] Ghaddar, N., Natural Convection Heat Transfer between a Uniformly Heated Cylindrical Element and its Rectangular Enclosure, *Int. J. Heat Mass Transfer, 35* (1992), 10, pp. 2327-2334
[6] Holzbecher, M., Steiff, A., Laminar and Turbulent Free Convection in Vertical Cylinders with Internal Heat Generation, *Int. J. Heat Mass Transfer, 38* (1995), 15, pp. 2893-2903
[7] Kao, P., Yang, R., Simulating Oscillatory Flows in Rayleigh-Benard Convection Using the Lattice Boltzmann Method, *Int. J. Heat Mass Transfer, 50* (2007), 17-18, pp. 3315-3328
[8] Zhou, Y., *et al.*, Numerical Simulation of Laminar and Turbulent Buoyancy-Driven Flows Using a Lattice Boltzmann Based Algorithm, *Int. J. Heat Mass Transfer, 47* (2004), 22, pp. 4869-4879
[9] Bau, H., Thermal Convection in a Horizontal Eccentric Annulus Containing a Saturated Porous Medium – An Extended Perturbation Expansion, *Int. J. Heat Mass Transfer, 27* (1984), 12, pp. 2277-2287
[10] Trisaksri, V., Wongwises, S., Critical Review of Heat Transfer Characteristics of Nanofluids, *Renewable and Sustainable Energy Reviews, 11* (2007), 3, pp. 512-523
[11] Wang, X., Mujumdar, A., Heat Transfer Characteristics of Nanofluids: A Review, *International Journal of Thermal Sciences, 46* (2007) 1, pp. 1-19
[12] Khanafer, K., *et al*., Buoyancy-Driven Heat Transfer Enhancement in a Two-Dimensional Enclosure Utilizing Nanofluids, *International Journal of Heat and Mass Transfer, 46* (2003), 19, pp. 3639-3653
[13] Eastman, J., *et al.*, Thompson, Anomalously Increased Effective Thermal Conductivities of Ethylene Glycol-Based Nanofluids Containing Copper Nanoparticles, *Appl. Phys. Lett., 78* (2001), 6, pp. 718-720
[14] Xie, H., *et al.*, Nanofluids Containing Multiwalled Carbon Nanotubes and Their Enhanced Thermal Conductivities, *J. Appl. Phys., 94* (2003), 8, pp. 4967-4971
[15] Choi, S. U. S., *et al.*, Anomalous Thermal Conductivity Enhancement in Nanotube Suspensions, *Appl. Phys. Lett., 79* (2001), 14, 2252
[16] Abu-Nada, E., Effects of Variable Viscosity and Thermal Conductivity of Cuo-Water Nanofluid on Heat Transfer Enhancement in Natural Convection, Mathematical Model and Simulation, *ASME J. Heat Transfer, 132* (2010), 5, pp. 1-9
[17] Abu-Nada, E., *et al*., Natural Convection Heat Transfer Enhancement in Horizontal Concentric Annuli Using Nanofluids, *Int. Commun. Heat Mass Transfer, 35* (2008), 5, pp. 657-665
[18] Habibi Matin, M., Pop, I., Natural Convection Flow and Heat Transfer in an Eccentric Annulus Filled by Copper Nanofluid, *International Journal of Heat and Mass Transfer, 61* (2013), June, pp. 353-364
[19] Shariat, M., *et al.*, Numerical Study of Two Phase Laminar Mixed Convection Nanofluid in Elliptic Ducts, *Applied Thermal Engineering, 31* (2011), 14-15, pp. 2348-2359
[20] Mirmasoumi, S., Behzadmehr, A., Numerical Study of Laminar Mixed Convection of a Nanofluid in a Horizontal Tube Using Two-Phase Mixture Model, *Applied Thermal Engineering, 28* (2008), 7, pp. 717-727

[21] Akbarinia, A., Behzadmehr, A., Numerical Study of Laminar Mixed Convection of a Nanofluid in Horizontal Curved Tubes, *Applied Thermal Engineering, 27* (2007), 8-9, pp. 1327-1337
[22] Kalteh, M., *et al.*, Experimental and Numerical Investigation of Nanofluid Forced Convection Inside a Wide Microchannel Heat Sink, *Applied Thermal Engineering, 36* (2012), Apr., pp. 260-268
[23] Habibi Matin, M., Pop, I., Numerical Study of Mixed Convection Heat Transfer of a Nanofluid in an Eccentric Annulus, *Numerical Heat Transfer, Part A: 65* (2014), 1, pp. 84-105
[24] Patankar, S., *Numerical Heat Transfer and Fluid Flow*, McGraw-Hill, New York, USA, 1980
[25] Teamah, M., *et al*., Numerical Simulation of Laminar Forced Convection in Horizontal Pipe Partially or Completely Filled with Porous Material, *International Journal of Thermal Sciences, 50* (2011), 8, pp. 1512-1522
[26] Teamah, M., El-Maghlany, W., Augmentation of Natural Convective Heat Transfer in Square Cavity by Utilizing Nanofluids in the Presence of Magnetic Field and Uniform Heat Generation/Absorption, *International Journal of Thermal Sciences, 58* (2012), Aug., pp. 130-142
[27] Teamah, M., El-Maghlany, W., Numerical Simulation of Double-Diffusive Mixed Convective Flow in Rectangular Enclosure with Insulated Moving Lid, *International Journal of Thermal Sciences, 49* (2010), 9, pp. 1625-1638
[28] Teamah, M., *et al.*, Numerical Simulation of Double Diffusive Laminar Mixed Convection in Shallow Inclined Cavities with Moving Lid, *Alexandria Engineering Journal, 52* (2013), 3, pp. 227-239

Paper submitted: August 2, 2014
Paper revised: October 19, 2014
Paper accepted: November 1, 2014